Molecular Therapy
Nucleic Acids
Original Article

An Antisense Oligonucleotide Leads to Suppressed Transcription of *Hdac2* and Long-Term Memory Enhancement

Shane G. Poplawski,[1,2,7] Krassimira A. Garbett,[3,7] Rebekah L. McMahan,[3] Holly B. Kordasiewicz,[4] Hien Zhao,[4] Andrew J. Kennedy,[5] Slavina B. Goleva,[6] Teresa H. Sanders,[3] S. Timothy Motley,[2] Eric E. Swayze,[4] David J. Ecker,[2] J. David Sweatt,[3] Todd P. Michael,[1,2] and Celeste B. Greer[3]

[1]J. Craig Venter Institute, La Jolla, CA, USA; [2]Ibis Biosciences and Abbott Company, Carlsbad, CA, USA; [3]Department of Pharmacology, Vanderbilt University, Nashville, TN, USA; [4]Ionis Pharmaceuticals, Carlsbad, CA, USA; [5]Department of Chemistry, Bates College, Lewiston, ME, USA; [6]Department of Molecular Physiology and Biophysics, Vanderbilt University, Nashville, TN, USA

Knockout of the memory suppressor gene histone deacetylase 2 (*Hdac2*) in mice elicits cognitive enhancement, and drugs that block HDAC2 have potential as therapeutics for disorders affecting memory. Currently available HDAC2 catalytic activity inhibitors are not fully isoform specific and have short half-lives. Antisense oligonucleotides (ASOs) are drugs that elicit extremely long-lasting, specific inhibition through base pairing with RNA targets. We utilized an ASO to reduce *Hdac2* messenger RNA (mRNA) in mice and determined its longevity, specificity, and mechanism of repression. A single injection of the *Hdac2*-targeted ASO in the central nervous system produced persistent reduction in HDAC2 protein and *Hdac2* mRNA levels for 16 weeks. It enhanced object location memory for 8 weeks. RNA sequencing (RNA-seq) analysis of brain tissues revealed that the repression was specific to *Hdac2* relative to related *Hdac* isoforms, and *Hdac2* reduction caused alterations in the expression of genes involved in extracellular signal-regulated kinase (ERK) and memory-associated immune signaling pathways. *Hdac2*-targeted ASOs also suppress a nonpolyadenylated *Hdac2* regulatory RNA and elicit direct transcriptional suppression of the *Hdac2* gene through stalling RNA polymerase II. These findings identify transcriptional suppression of the target gene as a novel mechanism of action of ASOs.

INTRODUCTION

Antisense oligonucleotides (ASOs) are clinically useful for treating a variety of diseases.[1] They employ base pairing with a target messenger RNA (mRNA) to achieve a high degree of selectivity. ASOs with stabilizing modifications (phosphorothioate and 2′-*O*-methoxyethyl) have been shown to reduce expression of their target genes in the central nervous system[2] for months after the last delivery of the drug.[3–5] The two most commonly reported mechanisms for ASOs in therapeutic applications are the following: (1) recruitment of RNase H1 to the RNA/ASO hybrid and subsequent degradation of the RNA[5] and (2) correction of splicing defects that lead to disease when the ASO is designed to target splice junctions.[6,7] Splicing occurs cotranscriptionally during the synthesis of RNA,[8–11] and this close link with transcription may suggest that ASOs could affect transcriptional synthesis. However, whether ASOs interfere with transcription has not yet been directly investigated.

Long-term memory formation and retention require coordinated transcriptional changes that are regulated by modifications to the epigenome. Decreasing acetylation by inhibiting histone acetyltransferases (HATs), such as cyclic AMP response element-binding (CREB)-binding protein (CBP), impairs long-term memory,[12–14] whereas increasing acetylation by inhibiting histone deacetylases (HDACs) enhances long-term memory.[15,16] Eleven isoforms of classical HDAC proteins exist in mammals. HDAC2 and HDAC3, in particular, are responsible for regulating synaptic plasticity and memory formation relative to other HDAC isoforms.[17,18] Conditional knockout of the *Hdac2* gene using *Nestin*-driven *Cre* expression in mice improves hippocampal and prefrontal cortex-dependent learning tasks, while not affecting locomotion.[17,19] Conditional knockout of *Hdac3* with the same *Nestin-Cre* conditional knockout is lethal in pups, leading to death soon after birth.[20] Because we were aiming to conduct sustained knockdown of a single *Hdac* isoform with ASOs, we chose to target *Hdac2*, reasoning that long-term repression of this isoform would likely be safer, potentially even early in development. Specific inhibition of HDAC2 has been a goal of pharmacological design,[21,22] but a completely selective inhibitor of HDAC2 catalytic activity has remained elusive because of poor pharmacokinetics and promiscuous subtype selectivity. ASOs represent a

Received 16 December 2019; accepted 21 January 2020;
https://doi.org/10.1016/j.omtn.2020.01.027.

[7]These authors contributed equally.

Correspondence: Celeste B. Greer, PhD, Department of Pharmacology, Vanderbilt University, 2220 Pierce Ave., RRB 424B, Nashville, TN 37232.
E-mail: celeste.greer@vanderbilt.edu
Correspondence: Todd P. Michael, PhD, J. Craig Venter Institute, 4120 Capricorn Ln., La Jolla, CA 92037.
E-mail: tmichael@jcvi.org

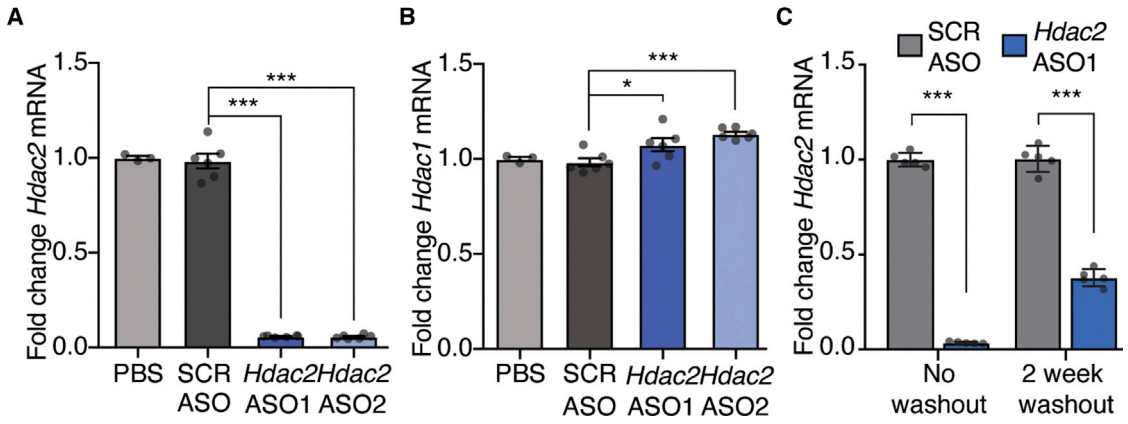

Figure 1. Specificity and Efficacy of *Hdac2*-Targeting ASOs in Primary Neuron Culture

(A) Fold change in *Hdac2* mRNA expression after 1 week, 10 μM ASO treatment. *Hdac2* expression was normalized to *Hprt* in mouse primary cortical neurons. (B) Same samples as used in (A) were tested with *Hdac1*-specific primers; n = 6 wells of cell culture from two biological replicates, each performed with 3 technical replicates. (C) Comparison of expression of *Hdac2* RNA after a continuous 16-day treatment or 2-day treatment with ASO, rinsing with media, replacing media, and incubating cells without ASO for 2 weeks; n = 5 wells of cell culture from two biological replicates, each performed with 2–3 technical replicates. Error bars represent ± standard error of the mean (SEM). Gray dots show relative expression values for individual replicates. One-way ANOVA with Dunnett's multiple comparisons post hoc test was used for (A) and (B), and two-way ANOVA with Sidak's multiple comparisons post hoc test was used for (C). *$p < 0.05$, ***$p < 0.001$. For qRT-PCR primers used throughout this study, refer to Table S1. See also Figure S1.

promising alternative to small molecule inhibitors of HDAC2 catalytic activity because of their specificity and longevity. Additionally, reduction of total HDAC2 protein levels with an ASO could be more therapeutically beneficial than only inhibiting catalytic activity because noncatalytic domains of HDAC2 suppress synaptic plasticity.[23] We previously designed an ASO targeting *Hdac2* mRNA. This *Hdac2* ASO elicited substantial memory enhancement in wild-type mice in object location memory tests, and it rescued impaired memory in a mouse model of autism.[24] However, the pharmacological characteristics of this ASO have been insufficiently explored.

We report here that our *Hdac2*-targeting ASO is long lasting and specific. A single injection of *Hdac2*-targeted ASO *in vivo* reduced *Hdac2* mRNA for 16 weeks and increased memory for 8 weeks. It has high selectivity for *Hdac2* but not other related histone deacetylase isoforms. Furthermore, it affects the expression levels of several other genes in the brain. These genes are involved in signaling through extracellular signal-regulated kinase (ERK) in the hippocampus and memory-associated immune signaling pathways in the forebrain. Although the *Hdac2* ASO used herein was designed to mediate degradation of target mRNA, we also found that the ASO elicits repression of an *Hdac2* regulatory post-transcription end-site RNA (post-TES RNA) transcript, which stimulates transcriptional suppression of its target gene and stalls RNA polymerase II (RNA Pol II).

RESULTS

Hdac2 ASOs Repress *Hdac2* mRNA in Cultured Cells

Cognitive enhancement functions of *Hdac2* have been ascribed predominantly to gene regulation in neurons,[17,25] so we first tested ASO-directed *Hdac2* knockdown in primary neuron cultures. Two *Hdac2*-targeting ASOs were tested. ASO1 targets the 3′ untranslated region (UTR), and ASO2 targets exon 10 of the *Hdac2* mRNA. Controls included the vehicle in which ASOs are diluted, phosphate-buffered saline (PBS), and a structurally similar scrambled (SCR) ASO that targets no known mouse genes. In primary neurons (Figure S1A), both *Hdac2* ASOs lead to *Hdac2* mRNA knockdown after 1 week of treatment relative to SCR ASO, measured by reverse transcription, followed by quantitative RT-PCR (qRT-PCR; Figure 1A). The ASOs also significantly reduced HDAC2 protein level (Figure S1B). Furthermore, the two *Hdac2* ASOs did not repress the mRNA of the closely related *Hdac1* isoform (Figure 1B). *Hdac1* was actually mildly increased in expression, which may be indicative of a compensatory mechanism.[26] Additionally, we confirmed the efficacy and specificity of the *Hdac2* ASOs in a mouse neuroblastoma Neuro2a (N2a) cell line differentiated with serum-starvation conditions (dN2a; Figure S1C). The *Hdac2* ASOs likewise reduced *Hdac2* (Figure S1D) but not *Hdac1* mRNA in this culture system (Figure S1E). These ASOs also specifically repress *Hdac2* in primary mixed glia culture, generated using methodology that promotes the growth of glia cells positive for markers of astrocytes and microglia (Figures S1F–S1H).[27,28] ASOs are reported to be long lasting in the brain, and to test if repression of *Hdac2* mRNA by *Hdac2* ASO1 is long lasting in primary neurons, we tested *Hdac2* mRNA expression, 14 days after washing out the ASOs and saw significant reduction persisting after the washout (Figure 1C). Based on these *in vitro* findings, we conclude these *Hdac2*-specific ASOs elicit specific *Hdac2* mRNA repression in several cell types, and this effect is long lasting in neurons.

Long-Term HDAC2 Protein Reduction in the Brain and Behavioral Memory Enhancement by *Hdac2* ASO1 *In Vivo*

After identifying the persistent knockdown elicited by the *Hdac2* ASO in neurons, we next tested the longevity of a single

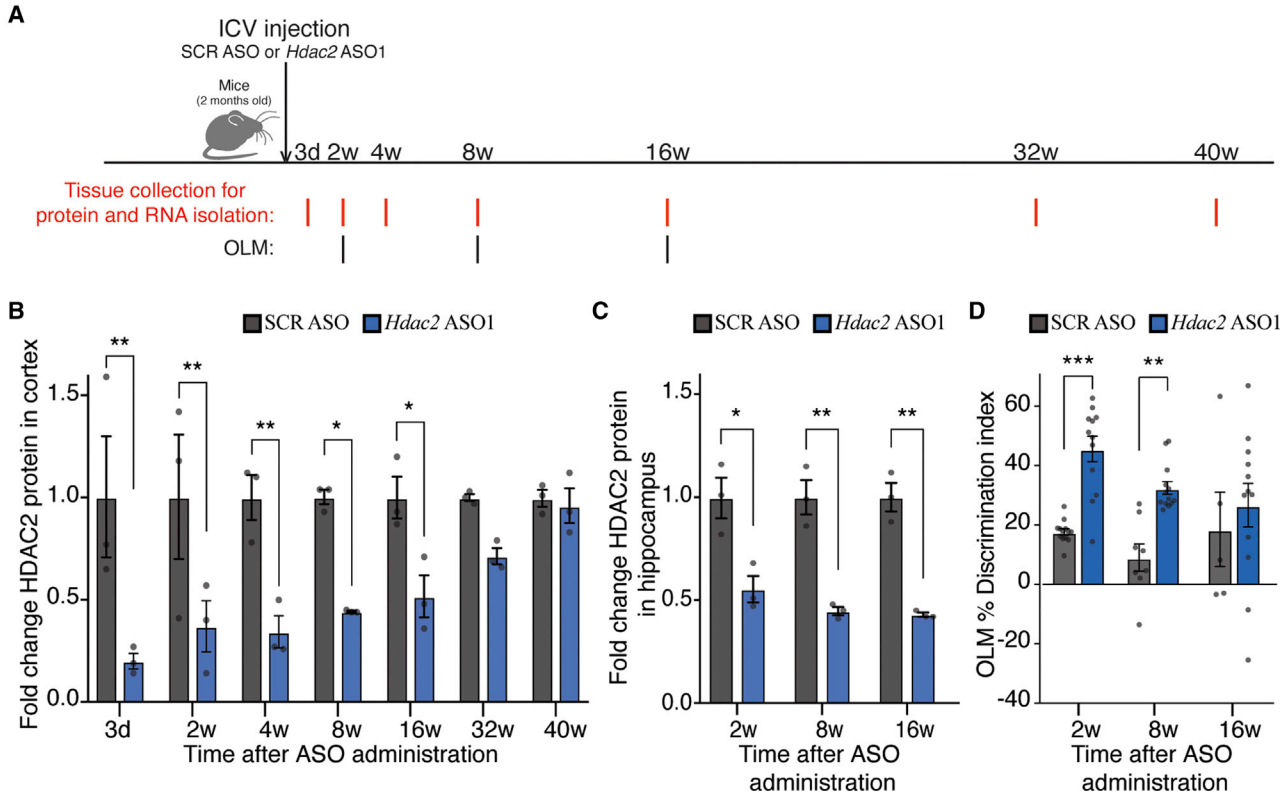

Figure 2. HDAC2 Protein Repression and Cognitive Enhancement across Time after ICV Injection of ASOs

(A) Timeline of the *in vivo* study. Tissue was collected to analyze protein and RNA for 3 mice treated with SCR ASO and 3 mice treated with *Hdac2* ASO1 at each time point. d, days; w, weeks. RNA analysis is displayed in subsequent figures. (B) Quantitation of HDAC2 protein in *Hdac2* ASO1 relative to SCR ASO from western blots of cortical samples. (C) Quantitation of amount of HDAC2 protein in the *Hdac2* ASO1 group relative to SCR ASO from western blots in hippocampus samples. (D) Discrimination index of OLM test for *Hdac2* ASO1 and SCR ASO groups; n = 13, 12, 8, 13, 5, and 12 (for each group left to right). Error bars represent ± SEM. *$p < 0.05$, **$p < 0.01$, ***$p < 0.001$ from two-way ANOVA with Sidak's multiple comparisons post hoc tests. Gray dots show values for individual replicates. Error bars represent ± SEM. See also Figure S2.

intracerebroventricular (ICV) injection of *Hdac2* ASO1 in mice. We examined molecular and behavioral changes in these animals relative to SCR ASO out to 40 weeks postinjection (Figure 2A). HDAC2 protein was significantly lower for *Hdac2* ASO1 compared to SCR ASO in the cortex from 3 days through 16 weeks after treatment (Figure 2B). The injection repressed HDAC2 protein expression in the hippocampus as well as at the three times tested, 2, 8, and 16 weeks (Figure 2C; Figure S2A). By contrast, protein analysis in the cerebellum showed no significant downregulation of HDAC2 protein levels at 2 and 32 weeks (Figure S2B).

Blocking HDAC2 has been shown to enhance memory formation, so we tested the duration of spatial memory enhancement in the ICV-injected mice. We used an object location memory (OLM) assessment of the treated animals at weeks 2, 8, and 16. Briefly, the OLM assessment is based on the spontaneous tendency of rodents to spend more time exploring an object that has been relocated. A higher discrimination index indicates that the mouse remembers the familiar placement. During training, we observe no difference in location preference between SCR ASO and *Hdac2* ASO1 animals (Figure S2C), and total object interaction time during the OLM test was not different between groups (Figure S2D). Animals that received a single ICV injection of *Hdac2* ASO1, 2 and 8 weeks later, had a higher discrimination index for the object in the new location compared to SCR ASO controls (Figure 2D). Because the cognitive enhancement decayed by 16 weeks, and HDAC2 protein levels were returning to normal, we ceased further testing of OLM after week 16.

To assess if this long-term effect by *Hdac2* ASO1 disturbed normal locomotion, we tracked movement during OLM training sessions at 8 and 16 weeks after injection and saw no differences in distance traveled (Figure S2E). An open-field experiment was previously conducted at 2 weeks postinjection, also showing no locomotion differences between SCR ASO and *Hdac2* ASO1.[24]

We further investigated if changes in other areas of the body were elicited by the ASOs and if the ASO crossed the blood-brain barrier. The liver, which is one of the primary peripheral sites of ASO accumulation,[29] showed no significant mRNA or protein reduction at the two time points tested (2 and 32 weeks) after ICV injection (Figure S2F).

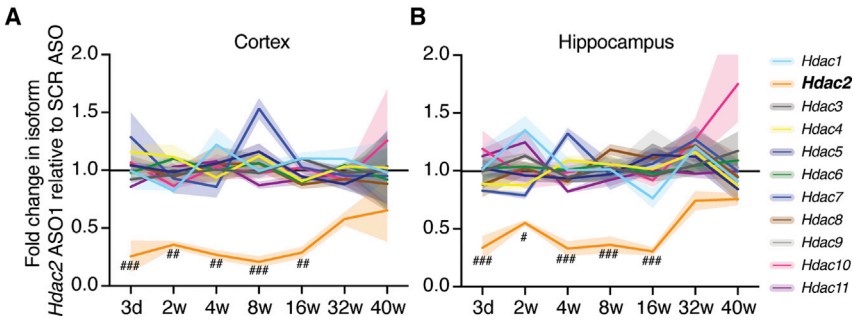

Figure 3. Isoform Specificity of *Hdac2*-Targeting ASOs in Different Brain Regions

Fold change in *Hdac* isoform expression for *Hdac2* ASO1 animals relative to SCR ASO animals from the equivalent time points after ICV. (A) Fold change in *Hdac2* mRNA level for *Hdac2* ASO1 relative to the SCR ASO group in RNA-seq of the cortex and (B) hippocampus. #FDR < 0.05, ##FDR < 0.01, ###FDR < 0.001. d, days; w, weeks after ICV infusion. Shaded areas represent ± SEM. See also Figure S3 and Tables S2, S3, and S4.

Similar to prior studies with other ASOs,[30,31] injection of *Hdac2* ASO1 into the tail vein did not repress *Hdac2* mRNA in the brain, suggesting the ASO does not cross the blood-brain barrier. However, we do see knockdown in the liver at 2 and 8 weeks in these intravenously (i.v.) injected animals (Figure S2G). These experiments emphasize that the ASO can improve memory, repress the intended target protein, and show favorable pharmacokinetics for targeting HDAC2 in the brain.

Isoform Specificity of *Hdac2*-Targeted ASOs

We sequenced RNA from our mouse tissue samples collected over the time course, which yielded sequences that aligned well to the mouse genome (Table S2). Principal component analysis shows low variance among replicates and clustering predominantly by brain subregion (Figure S3A). We examined the isoform specificity of *Hdac2* ASO1 *in vivo* using these datasets. Of the 11 isoforms of classical *Hdacs*, the *Hdac2* gene was the only isoform significantly changed at any time during the 40 weeks of the study in the cortex (Figure 3A) and hippocampus (Figure 3B). In these subregions, repression of *Hdac2* was significant from 3 days to 16 weeks post-injection. Even though protein levels of HDAC2 were unchanged in the cerebellum, we nonetheless analyzed mRNA by RNA sequencing (RNA-seq). It also revealed significant knockdown of *Hdac2* but not other *Hdac* isoforms (Figure S3B). Like in the cortex and hippocampus, the changes were statistically significant between 3 days and 16 weeks after administration of the ASOs, but mean *Hdac2* mRNA levels never fell below 50% of SCR ASO levels, so repression was comparatively milder in this brain region. Together, these data emphasize that the *Hdac2* ASO is extremely isoform specific.

Gene-Expression Changes Induced by *Hdac2* ASO1 *In Vivo*

Next, we wanted to identify gene-expression changes induced by *Hdac2* ASO1 during memory enhancement. This would generate new hypotheses regarding transcriptional programs that elicit cognitive enhancement when HDAC2 protein is reduced. The longevity of *Hdac2* ASO1 action allowed us to look at changes occurring after long-time periods of sustained repression that are not possible to study *in vitro*. We identified significantly changed genes by *Hdac2* ASO1 during the time span when we saw significant cognitive enhancement (Figure 2D). We did this by analyzing RNA-seq data from all time points collected between 2 and 8 weeks after ICV together (2, 4, and 8 weeks) and identifying a set of genes with altered expression by *Hdac2* ASO1 relative to SCR ASO. In the cortex, differentially expressed genes were predominantly activated by *Hdac2* ASO1 during cognitive enhancement (Figure 4A, left). For this set of genes, we also looked at fold changes at each time point (Figure 4A, right). By the times when HDAC2 protein levels are no longer significantly suppressed at 32 and 40 weeks (Figure 2B), the magnitude of fold changes in this gene set decays. The identified genes with altered expression in the cortex during cognitive enhancement are involved in immune-system processes, major histocompatibility (MHC) class I and II signaling, tumor necrosis factor (TNF) production, cell adhesion, and angiogenesis (Figure 4B). In the hippocampus, like in the cortex, genes are predominantly activated during cognitive enhancement. A similar pattern of activation and then eventual decay is seen (Figure 4C). Many of the same gene pathways as the cortex were identified, since of the 153 significantly changed genes, 97 overlap, but Gene Ontology (GO) terms related to positive regulation of ERK signaling cascades and regulation of neuron projections also were significantly enriched for this gene set (Figure 4D). In the cerebellum, 80 genes were differentially expressed between SCR ASO- and *Hdac2* ASO1-treated animals. Unlike in the cortex and hippocampus, genes were predominantly repressed rather than activated by *Hdac2* ASO1 (Figure S4A), and overlap with differentially expressed genes from the hippocampus and cortex is low (Figure S4B). No biological process gene ontology pathways were significantly enriched in this set of genes.

Many of the genes identified in the cortex and hippocampus are involved in immune responses. Signaling through immune pathways is important for memory formation,[32] so it is possible that the activation of these pathways leads to procognitive effects. However, activation of inflammation can also inhibit memory, neurogenesis, and neuroplasticity through decreasing brain-derived neurotrophic factor (BDNF).[33–35] Therefore, we checked levels of BDNF protein in hippocampus from 2 to 8 weeks and saw no difference in BDNF protein levels between SCR ASO- and *Hdac2* ASO1-treated animals (Figure S4C), suggesting *Hdac2* ASO1 is not activating cytokine signaling in a manner previously reported to interfere with neuroplasticity.

To validate the identified changes with qRT-PCR, we picked eight genes activated in the cortex and hippocampus that represented

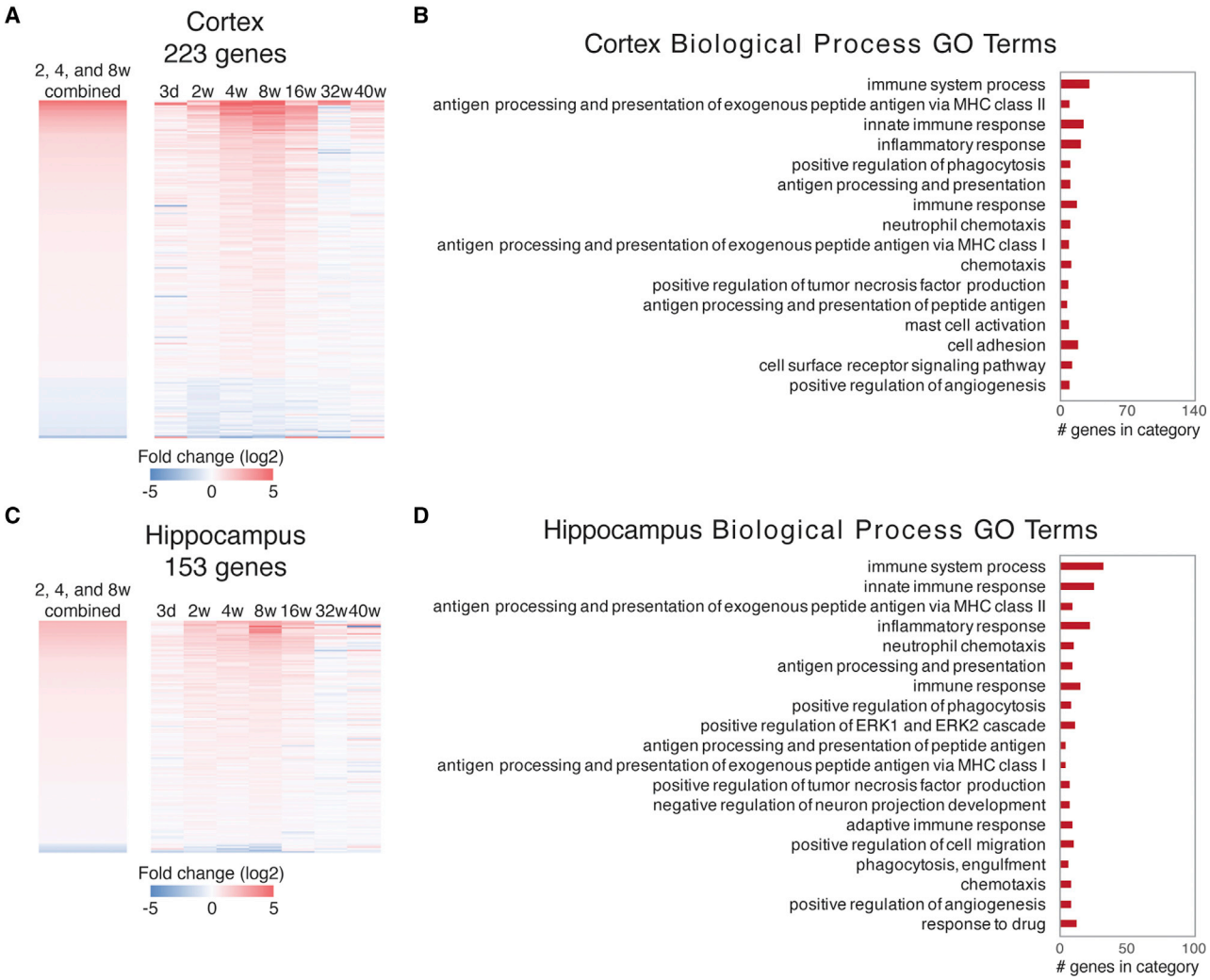

Figure 4. Functions of Significantly Changed Genes by *Hdac2* ASO1 Relative to SCR ASO in the Cortex and Hippocampus during Memory Enhancement

(A) Heatmap of fold changes between *Hdac2* ASO1 and SCR ASO in RNA-seq for differentially expressed genes during cognitive enhancement (2-, 4-, and 8-week combined analysis; n = 9 for each treatment; FDR < 0.05) in the cortex. Significantly changed genes were sorted in decreasing order by fold change in the combined 2-, 4-, and 8-week analysis. To the right, fold changes at individual time points are shown for the same set of genes sorted in the same order. Red represents activation, and blue represents repression. d, days; w, weeks. See Table S6 for the list of these differentially expressed genes in the cortex during cognitive enhancement. (B) DAVID GO biological process terms generated from significantly changed genes in the cortex are ranked top to bottom from most to least significant. Bonferroni p value < 0.05 was the cut-off. (C) Heatmap of significant expression changes and (D) DAVID GO for differentially expressed genes in the hippocampus were analyzed, as described for the cortex. See Table S7 for the list of these differentially expressed genes in the hippocampus during cognitive enhancement. See also Figure S4.

several of the subcategories identified in the GO analysis. We confirmed activation of all eight in RNA isolated from 2-, 4-, and 8-week hippocampus samples (Figure S4D). Next, we tested if expression of these genes is altered in cultured neurons treated with ASOs. Of the set of eight, only *S100a4*, a calcium-binding protein, was activated by *Hdac2* ASO1 in neuron cultures (Figure S4E). Furthermore, we find no significant changes in glia cultures in these genes (Figure S4F), suggesting that either *Hdac2* ASO1 affects gene expression in cell types not represented in these cultures or that a complex interaction of cell types in the brain could be the source of these changes *in vivo*.

Prior work has shown that *Hdac2* knockdown with short hairpin RNA (shRNA) in primary neuron cultures activates the expression of a set of genes involved in synaptic function.[23] We looked at the expression of these twelve genes in our RNA-seq datasets and found that none of them was significantly changed in the cortex (Figure S4G) or hippocampus (Figure S4H) between 2 and 8 weeks or at any individual time point. qRT-PCR, of a set of six genes selected from this group, confirms the lack of activation by *Hdac2* ASO1 in the 2-, 4-, and 8-week hippocampus samples (Figure S4I). Our RNA-seq was conducted in heterogeneous tissue, so we cannot rule out that these genes could be changed in specific

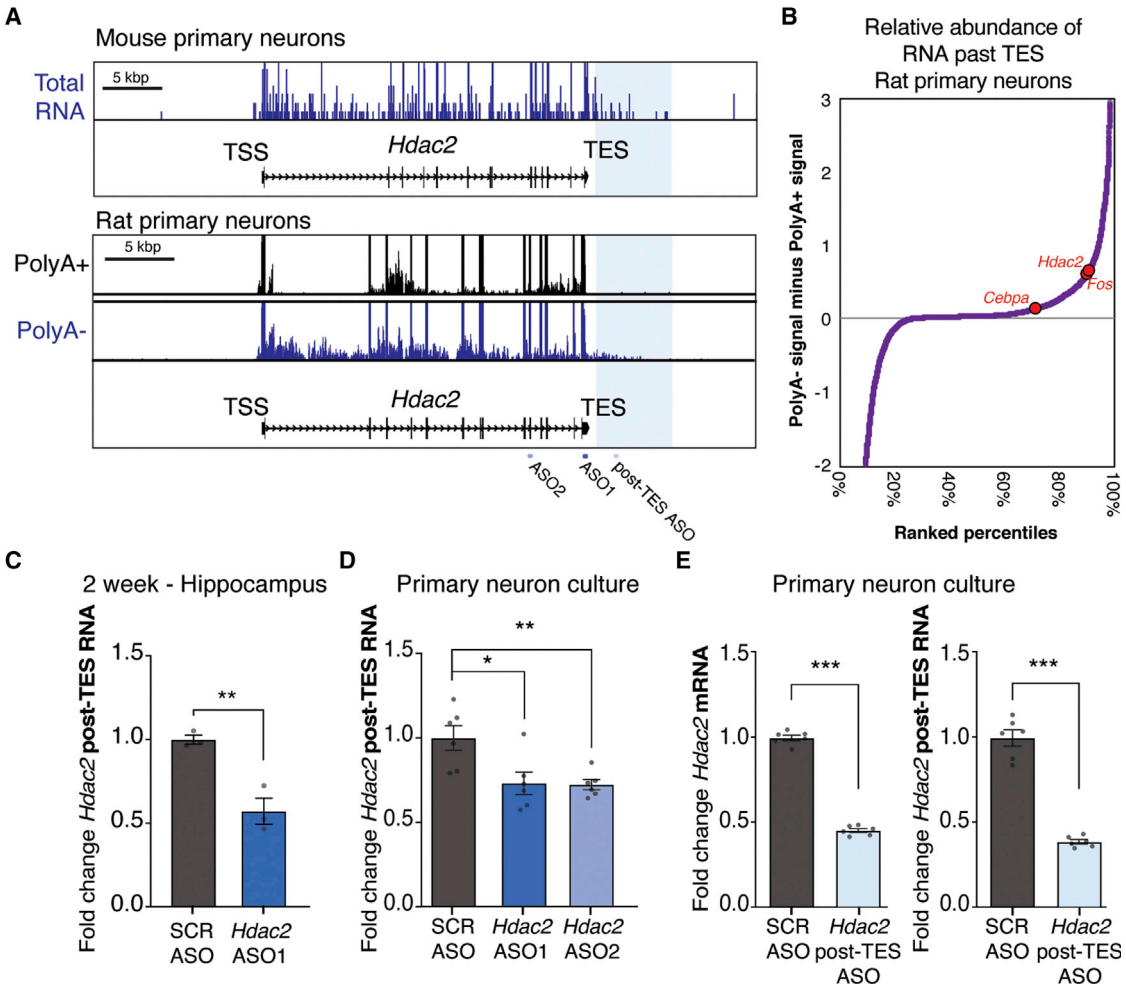

Figure 5. *Hdac2* Is Regulated by a Nonpolyadenylated Transcript that Extends beyond the TES that *Hdac2* ASOs Repress

(A) RNA-seq reads at the *Hdac2* gene from indicated sequencing libraries. Reads were stranded, and only the reads representing sense transcripts relative to the direction of the *Hdac2* gene are shown (+ for mouse, − for rat). Gene tracks are oriented such that the 5′ end of the *Hdac2* transcript is seen on the left. Locations of ASO target sequences are indicated below the diagrams. Region past the annotated TES +500 to +6,000 bp used in (B) is shaded in blue. (B) Signal in the sense direction in polyA$^-$ RNA-seq past annotated TES (+500 to +6,000 bp downstream) was determined, the polyA$^+$ signal was subtracted, and genes were plotted in rank order of least to most signal. The positions of *Hdac2* and other genes suspected or validated to have regulatory ecRNAs are labeled within this ranking. (C) Signal from RNA generated beyond the TES was detected with qRT-PCR using primers designed to the 3′ end of the *Hdac2* post-TES transcript (1.4 kb pairs [kbp] beyond the TES) in mouse hippocampus 2 weeks after ICV; n = 3 animals. (D) Post-TES signal after treatment with ASOs in primary neurons; n = 6 wells of cell culture from 2 biological replicates done in triplicate. (E) The *Hdac2* post-TES ASO repressed *Hdac2* mRNA (left) and *Hdac2* post-TES RNA expression (right). Reverse transcription of RNA was done with random primers for (C)–(E); n = 6 wells of cell culture from 2 biological replicates done in triplicate. *Hdac2* mRNA and post-TES signal were normalized to *Hprt*. Error bars represent ± SEM. Gray dots show values for individual replicates. *p < 0.05, **p < 0.01, ***p < 0.001 by one-way ANOVA with Dunnett's multiple comparisons post hoc test in (D) or Student's t tests in (C) and (E). See also Figure S5.

nonabundant cell types. However, we also do not see changes in these genes in primary neurons treated with *Hdac2* ASO1 either (Figure S4J). Although differences in the knockdown method or culture preparation could explain our dissimilar findings, our cultures more closely match our *in vivo* data for this subgroup of genes. In summary, *Hdac2* ASO1 elicited a restricted set of changes in mRNA transcript abundance, predominantly affecting genes with ascribed functions in immune signaling in the cortex and hippocampus.

ASOs Repress a Nonpolyadenylated *Hdac2* Sense Transcript that Promotes *Hdac2* mRNA Expression

The long-lasting nature of the ASO repression in neurons and in brain tissues made us question if the ASO only degrades *Hdac2* mRNA or if it might also block its synthesis. We noticed in sequencing datasets that nonpolyadenylated transcription at the *Hdac2* locus continues in regions beyond the annotated transcription end site in primary neurons from mice[36] and rats[37] (TES; Figure 5A). Previous work has demonstrated that extra-coding RNAs (ecRNAs)

are generated from many protein-coding genes in neurons and promote their transcription.[37,38] These RNAs are sense transcripts that are unspliced and transcribe over mRNA sequences and prevent repression of their gene of origin. ecRNAs begin transcription upstream of the transcription start site (TSS) and terminate downstream of the TES of the gene they regulate. *Cebpa* and *Fos* have regulatory ecRNAs, so we compared their post-TES sense transcript levels to *Hdac2* and identified post-TES signal for all genes. *Hdac2* is in the top 10% of all genes for having post-TES transcription (Figure 5B) and exhibits more of this post-TES transcription than *Fos* or *Cebpa*. This suggests that *Hdac2* could be regulated by a putative ecRNA.

Because the ASO1 and ASO2 target sequence is present in the *Hdac2* mRNA, *Hdac2* pre-mRNA, and putative *Hdac2* ecRNA (Figure 5A; target sequence location indicated below gene tracks), we wanted to test if these ASOs repress levels of the transcript that extend beyond the TES. We analyzed total RNA from the hippocampus, 2 weeks post-ICV, reverse transcribed with random primers, rather than with oligo dT, which would only pick up polyadenylated transcripts. We found that the post-TES transcript was repressed by *Hdac2* ASO1 *in vivo* (Figure 5C). Likewise, in primary cortical neurons, *Hdac2* post-TES transcript expression was reduced by both *Hdac2* ASO1 and ASO2 (Figure 5D). The mean abundance of *Hdac2* mRNA relative to the *Hdac2* post-TES transcript is over 100-fold in primary neurons and hippocampus (Figure S5A), meaning the post-TES transcript is relatively limited in quantity in total RNA preparations. To see if repressing only the putative ecRNA by targeting a region past the TES had an effect on *Hdac2* expression, we designed a post-TES-specific ASO. This post-TES ASO significantly reduced *Hdac2* mRNA (Figure 5E, left) and the post-TES transcript (Figure 5E, right). Despite the low relative abundance of *Hdac2* post-TES transcript to *Hdac2* mRNA, targeting only the post-TES transcript had a powerful effect on the much more abundant *Hdac2* mRNA. From these data, we conclude that *Hdac2* mRNA and the post-TES transcript are both efficiently downregulated by *Hdac2*-targeting ASOs, and solely targeting the post-TES region that is unique to a putative ecRNA transcript is sufficient to elicit mRNA repression.

Prior reports show,[37] and we confirmed, that *Fos* ecRNA-targeting ASO that targets the post-TES region of *Fos* reduces *Fos* mRNA transcript levels (Figure S5B). We furthermore found, like our *Hdac2* mRNA-targeting ASOs, that a *Fos* mRNA-targeting ASO downregulates the expression of *Fos* ecRNA (Figure S5C), suggesting that targeting mRNA sequences can also disrupt ecRNA expression. Mechanistically, this means that for both *Hdac2* and *Fos*, a single mRNA-targeting ASO may complete two tasks that both lead to downregulation of the target: transcriptional suppression through regulatory RNA knockdown and degradation of mRNA via RNase H1. Moreover, because *Hdac2* and *Fos* ASOs are both capable of being repressed using a post-TES ASO, these dual mechanisms could possibly be utilized to potently target other genes that have nonpolyadenylated post-TES regulatory transcripts with ASOs, which from our estimates includes about one-quarter of genes in neurons.

Direct Transcriptional Suppression by ASOs

Since ecRNAs are reported to regulate transcriptional accessibility, we tested the hypothesis that ASOs affect the transcription of *Hdac2* pre-mRNA. First, to assess the possibility of a transcriptional suppression mechanism *in vivo*, using random primer-generated cDNA made from total RNA taken from hippocampus samples from 2 weeks post-ICV, we confirmed that *Hdac2* mRNA is knocked down using our primers that span an exon-exon junction (Figure 6A, left). Moreover, at regions of the *Hdac2* gene that are part of the processed transcript (exon 5 and 3′ UTR), the knockdown level is similar to that of *Hdac2* mRNA (Figure 6A, right). This suggests that the processed transcript is evenly repressed, and no splicing defects occur. Indeed, looking at our sequencing data for the 2-week post-ICV samples, each exon of *Hdac2* is repressed to a similar level (between 40% and 60% of SCR ASO levels) across the gene by *Hdac2* ASO1 (Figure S6A). However, in regions of the gene corresponding to the nascent pre-mRNA or putative ecRNA (intron 1 and intron 12), there is uneven repression (Figure 6A, right). Repression occurs more so in the gene body, as indicated by reduction of signal from *Hdac2* intron 12, rather than in the promoter-proximal region of *Hdac2* intron 1.

To directly test if ASO1 and ASO2 prevent *Hdac2* pre-mRNA production, we conducted nuclear run-on (NRO) experiments to quantify nascent *Hdac2* transcripts. During NRO, newly synthesized RNA is tagged with bromouridine (BrU) and purified by immunoprecipitation (IP). The IP method was optimized to be able to isolate BrU-labeled RNA (+ samples), while washing away unlabeled RNA (− samples) with a very low background signal (Figure 6B). The level of *Hdac2* pre-mRNA in the immunoprecipitated nascent RNA fraction was measured by qRT-PCR. We observed that *Hdac2* ASO1 treatment results in no change at intron 1, a trend for reduced transcription past intron 1, and significant reduction of transcription in the 3′ UTR of *Hdac2* in primary neurons (Figure 6C). In dN2a cells, there was a similar pattern in the gene body past intron 1 with significant repression in the 3′ UTR, and *Hdac2* ASO2, although it targets a different exon, repressed *Hdac2* transcription in a similar pattern as ASO1 (Figure 6D).

Inhibitors of HDAC catalytic activity can activate and repress transcription,[39,40] so we tested if the changes we observed in the NRO experiment were an indirect effect of blocking HDAC activity using two broad-spectrum HDAC inhibitors: sodium butyrate (NaBu) and suberoylanilide hydroxamic acid (SAHA). There was no repression of *Hdac1* or *Hdac2* transcript levels (Figure S6B), and *Hdac2* transcription in NRO assays was not blocked by NaBu (Figure S6C). Treatment of the cells with SAHA also did not reduce *Hdac2* transcript levels but actually increased *Hdac1* and *Hdac2* mRNA expression (Figure S6D). These controls suggest that *Hdac2* ASOs block transcription of *Hdac2*, irrespective of any epigenetic changes resulting from inhibition of deacetylation.

Transcription is not repressed in intron 1 by *Hdac2* ASO1 *in vivo* or *in vitro*, so we hypothesized that the ASO may interfere with the ability of RNA Pol II to continue transcription in the gene body after

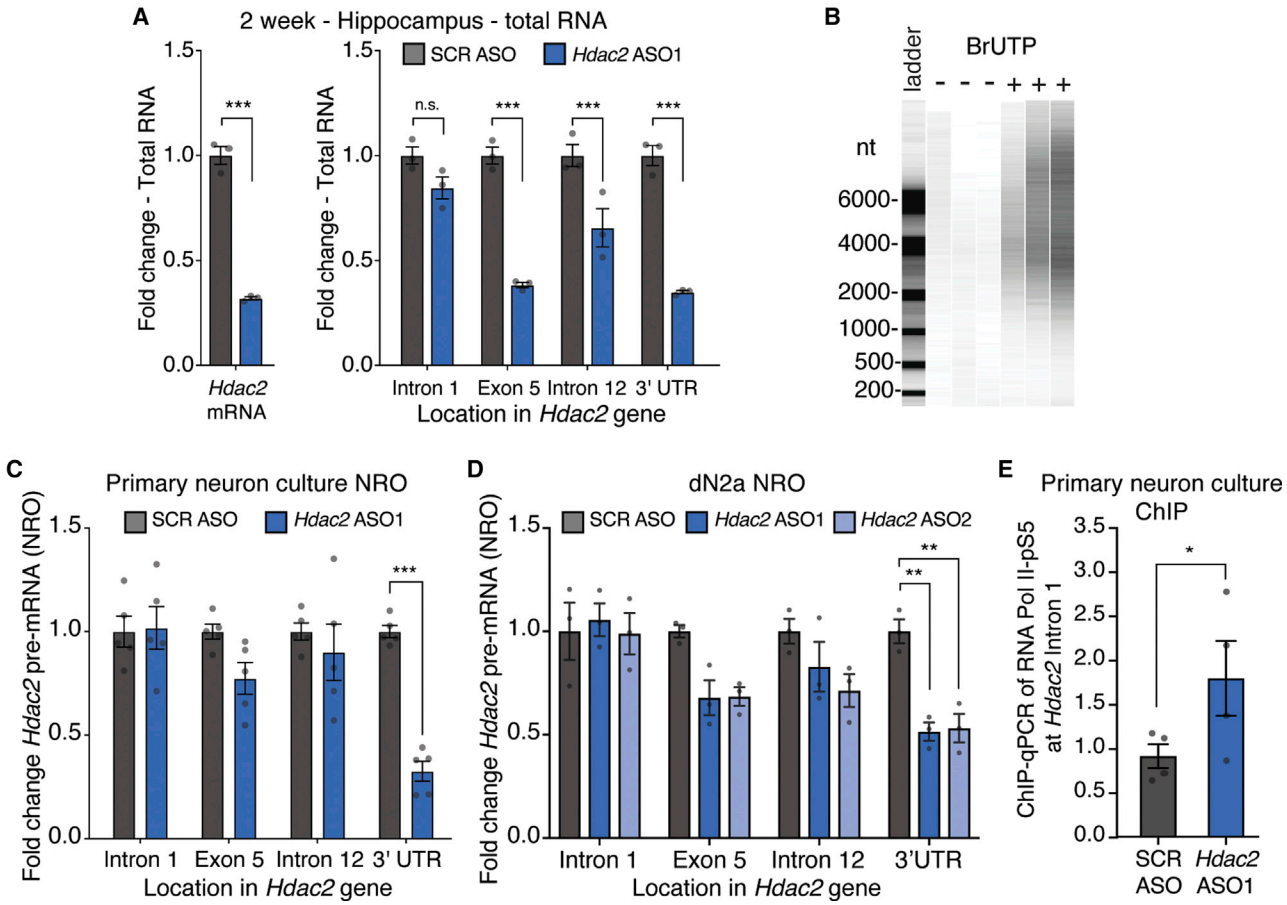

Figure 6. Direct Repression of *Hdac2* Transcription by *Hdac2* ASOs

(A) Expression of *Hdac2*-processed mRNA transcript in mouse hippocampus, 2 weeks post-ICV, detected after random primer reverse transcription (left) and expression of regions across the *Hdac2* gene in the same samples (right). (B) Bioanalyzer high-sensitivity RNA chip gel-like image of BrUTP antibody-immunoprecipitated NRO samples made with unlabeled UTP (−) or with BrUTP (+). Units for ladder are shown in nucleotides (nt). (C) qRT-PCR of NRO samples made from primary cortical neurons treated with ASOs; n = 5 biological replicates from independent preparations of primary neurons. (D) qRT-PCR of NRO samples made from dN2a cells treated with ASOs; n = 3 technical replicates. (E) ChIP-qPCR with RNA Pol II-pS5 antibody was conducted in primary neurons treated with SCR ASO and *Hdac2* ASO1; n = 4 biological replicates. Paired Student's t test. Two-way ANOVA with Sidak's multiple comparisons post hoc test was performed for (A), (C), and (D). Error bars represent ± SEM; gray dots show values for individual replicates. *p < 0.05, **p < 0.01, ***p < 0.001. See also Figure S6.

initiating transcription. When RNA Pol II stalls, the initiated form accumulates near the promoter.[41,42] Therefore, we looked for an accumulation of the initiated form of RNA Pol II (RNA Pol II phosphorylated at serine 5 of the C-terminal domain repeat region [RNA Pol II-pS5])[43,44] in intron 1 using chromatin immunoprecipitation (ChIP)-qPCR in primary neurons after *Hdac2* ASO1 treatment. We found more binding of this active form of RNA Pol II at this location after *Hdac2* ASO1 treatment (Figure 6E), as is expected for stalled RNA Pol II. Therefore, we conclude that *Hdac2* ASOs can reduce transcription of their target gene.

DISCUSSION

Conditional knockout of *Hdac2* in the brain elicits memory enhancement, while not affecting locomotion[17] or anxiety.[17,19] This makes it an attractive target for sustained repression, and our studies indicate that *Hdac2* ASOs provide a powerful avenue to generate long-lasting beneficial changes in epigenomic organization in the central nervous system. Like HDAC3-specific inhibitors,[45] we find that blocking *Hdac2* expression leads to cognitive enhancement in wild-type mice, indicating that suppression of single HDAC isoforms can be beneficial for improving long-term memory.[17,18] Prior studies show that the targeting of *Hdac2* specifically can ameliorate cognitive and social aspects of autism spectrum disorders.[24,46] Moreover, overexpression of HDAC2 protein is observed in human Alzheimer's disease, and memory improves after *Hdac2* knockdown in an animal model of Alzheimer's disease.[47] Together, this shows that specific HDAC2 reduction is potentially therapeutically useful, and because of the chronic nature of these conditions, a long-lasting treatment, such as the described *Hdac2*-specific ASO, would be desirable.

We conducted unilateral ICV injection to administer the ASOs in this study. Regardless of the site of entry, ASOs are distributed widely in the brain after being introduced to the cerebrospinal fluid. Intrathecal (IT) injection is used more commonly in human and nonhuman primate studies.[48] Bolus IT injection in nonhuman primates into the cerebrospinal fluid has been shown to spread effectively to various distal brain regions, including the cortex and hippocampus.[48,49] Therefore, injections of ASOs that penetrate the blood-brain barrier lead to wide distribution in the central nervous system. This seems to be true in our mice, too, because the RNA knockdown we report in the RNA-seq experiment was measured in the opposite hemisphere as the ventricle where the ASO was injected. What remains unknown is whether ASOs are broken down, sequestered, or cleared from the brain. Although the mechanisms of cellular uptake of ASOs have been studied and reviewed,[29] the methods by which the body removes ASOs are much less understood beyond which organs participate. This is especially unclear in the central nervous system as intact ASOs do not seem to cross the blood-brain barrier, at least to a sufficient level to elicit therapeutic benefit. More exploration of how ASO targets recover expression and how ASOs leave the brain would be helpful for understanding the pharmacology of ASOs.

We do not yet fully understand which transcriptional changes elicited by long-term suppression of HDAC2 levels are necessary for memory enhancement. However, we find that ASO-induced repression of HDAC2 is associated with secondary changes in the expression of gene networks in the brain that have previously been implicated in forming memories. For example, genes associated with ERK signaling are altered in the hippocampus after lowering HDAC2 expression, and this signaling pathway is essential for memory formation and long-term potentiation of synaptic activity.[50,51] We also see changes in genes associated with immune functions in the hippocampus and cortex. Genes of this functional category play a role in promoting cognition[52,53] and synaptic plasticity.[54–57] MHCI proteins are involved in memory[52] and synapse formation.[58] Likewise, evidence suggests that genes related to MHCII are also involved in learning.[53] RNA-seq-identified positive regulation of TNF production as a significantly enriched set of genes changed after *Hdac2* ASO1 treatment, and *Tnfrsf1a*, which encodes the TNF1a receptor, is increased in the cortex and hippocampus. Importantly, TNF1a can increase synaptic strength through modulating α-amino-3-hydroxy-5-methyl-4-isoxazolepropionic acid receptor (AMPAR) trafficking.[59] Several more individual genes identified in our RNA-seq experiments also point to possible roles in aiding cognition. The S100A proteins bind calcium, and we found that the *S100a4* gene was activated by *Hdac2* ASO1 in the hippocampus and cortex and in primary neuron cultures. *S100a4* promotes neurite outgrowth,[60] protects neurons after injury,[61,62] and decreases Aβ aggregation.[63,64] S100 proteins are secreted at sites of inflammation,[65] so like several of the genes identified, they also seem to have immune functionality. The cluster of differentiation 74 (*Cd74*) gene was also activated in the cortex and hippocampus by *Hdac2* ASO1, and the CD74 protein is involved in assembly and trafficking of MHCII.[66] Increasing *Cd74* expression decreases Aβ load and improves memory in Alzheimer's disease model mice.[67] In whole, these results point to needing a better understanding of the multifaceted roles immune-related genes play to fully understand their role in synaptic activity and forming memories.

ASOs can be designed to use several mechanisms of altering gene expression through modulating stability, splicing, and translation of mRNA.[68] Our study reveals a yet another mechanism of directly blocking transcriptional progression across the gene. Transcription-promoting noncoding RNAs, like ecRNA and enhancer RNAs, alter the accessibility of DNA to RNA Pol II.[37,38,69] The nonpolyadenylated post-TES transcript of *Hdac2* that is potentially part of an *Hdac2* ecRNA could reduce accessibility after it is reduced by the ASO. This may explain the halt in RNA Pol II progression across the *Hdac2* gene. This is consistent with our findings that a post-TES targeting ASO reduces *Hdac2* mRNA and that the transcription stall is upstream of the ASO target site. The direct block of *Hdac2* transcription could help explain the endurance of effect for a single application of ASO. It appears that at least one-quarter of genes has a sufficient post-TES signal to be a potential candidate for this repression strategy. ASOs elicit a targeted reduction in gene expression that is potent and long lasting but accomplishes this without altering the underlying DNA sequence. This makes ASOs more attractive than other gene therapy approaches, like CRISPR,[70] in certain contexts. This is because the changes induced by ASOs are extremely specific and enduring but not permanent or damaging to genomic sequences.

MATERIALS AND METHODS

ASOs

Hdac2 ASO1 (5′-CToCoAoCTTTTCGAGGTToCoCTA-3′), *Hdac2* ASO2 (5′-AToGoCoAGTTTGAAGTCToGoGTC-3′), *Hdac2* post-TES ASO (5′-CCoCoAoAATCACCTGTTCoToGAA-3′), and non-targeting SCR ASO (5′-GToToToTCAAATACACCToToCAT-3′) were generated by Ionis Pharmaceuticals using the phosphorothioate and 2′-*O*-methoxyethyl-modified ASO platform. *Fos* ASOs (*Fos* mRNA ASO [5′-UCUGUCAGCTCCCTCCUCCG-3′], *Fos* ecRNA ASO1 [5′-AGAUUGGCTGCTTGGUGGGU-3′], *Fos* ecRNA ASO2 [5′-ACUAGCGTGTCCTCTGAGUGA-3′], and nontargeting SCR ASO [5′-GUUUUCAAATACACCUUCAU-3′]) were ordered from Integrated DNA Technologies (IDT). Sequences are designed for targeting mouse transcripts. Underlined residues are deoxynucleosides, and all others are 2′-*O*-methoxyethyl nucleosides. All linkages are phosphorothioate, except those indicated by "o" between residues, which are phosphodiester.

Cell Culture

Primary cortical neuron cultures were made from neonatal (P0) mice. Dissected cortices were treated with papain, supplemented with cysteine, and triturated to dissociate neurons. Cells were passed through a 70-μm filter (Falcon) and plated with neurobasal complete media (neurobasal with 1× B27 supplement, 1 mM sodium pyruvate, 1 mM HEPES, 100 U/mL penicillin, 100 μg/mL streptomycin, and 0.5 mM L-glutamine) plus 10% fetal bovine serum (FBS). On day *in vitro* 1 (DIV 1), media were changed to neurobasal complete

without FBS. Cells were treated overnight with 4 μM 5-fluoro-2′-deoxyuridine (FdU) to minimize dividing cells on DIV3, and 10 μM ASO was applied on DIV 5. For washout experiments, neurons were treated for 2 days with 10 μM ASO from DIV 5–7. Cells were rinsed with complete neurobasal media, left a few minutes, and media were replaced again. One-half of the media changes was done every 2 to 3 days for all primary neuron culture experiments. New media for changes did not contain ASO. All primary neuron experiments were performed using neurons at DIV 12–21. Time for neuron maturation did not affect gene-expression changes observed (Figure S4), so data were combined.

N2a cells were obtained from ATCC and grown according to their recommended conditions. For long treatments, plates were coated in poly-L-lysine. Cells attached overnight, and media were changed to differentiation media (DMEM with L-glutamine without glucose, 10 mM galactose, 100 U/mL penicillin, 100 μg/mL streptomycin, and 1× N2 supplement) to make dN2a. After 4 days, one-half of the media was changed and supplemented with complete neurobasal media at a ratio of 1:400 neurobasal to differentiation media. One-half of the media changes was done as needed. Replacement media contained the drug at the same concentration as the initial treatment.

Primary glia cells were collected from pups, as described for primary neurons, except cells were plated at 10× less density and were grown in DMEM plus 100 U/mL penicillin, 100 μg/mL streptomycin, and 10% FBS past DIV 1.[27] No FdU was applied, and one-half of the media changes was done every 2 to 3 days. 10 μM ASO was added on DIV 3, and ASO was added at the same dose to media during one-half of the media changes.

For *Fos* ecRNA experiments, N2a were transfected with GenMute reagent (SignaGen), according to the manufacturer's specifications, with ASO at a final concentration of 60 nM. Media were changed to differentiation media, 5 h after transfection, and 2 days later, changed to neurobasal media. RNA was extracted the following morning.

Mice

Male B6129S F1 hybrid mice at 2 months of age were used in this study. This strain was acquired from The Jackson Laboratory. All procedures were performed with Institutional Animal Care and Use Committee (IACUC)-approved protocols and conducted in full compliance with the Association for Assessment and Accreditation of Laboratory Animal Care (AAALAC).

Targeted Gene-Expression Analysis

For all tissue-culture samples and 2-week hippocampus samples that were analyzed by random priming, the RNeasy Plus Kit (QIAGEN) and SuperScript VILO (Invitrogen) were used, according to the manufacturers' instructions. For RNA-seq qRT-PCR validation, 500 ng of RNA from 2-, 4-, and 8-week hippocampus samples was reverse transcribed with the Bio-Rad iScript Synthesis Kit, as recommended by the manufacturer. qPCR was performed with the CFX96 Optical Reaction Module (Bio-Rad) using SYBR Green (Bio-Rad). Relative gene expression was determined using the ΔΔCt method[71] and normalized to *Hprt* for *in vitro* experiments and *Gapdh* for *in vivo* experiments. qPCR primer sequences are listed in Table S1.

In Vivo ASO Administration

ASOs were injected into the brain by a unilateral ICV bolus injection of 300 μg. Mice were anesthetized with 2% isoflurane and secured in a stereotaxic frame (David Kopf Instruments). ASOs were diluted to 60 μg/μL in saline and injected 15 mg/kg into the lateral ventricle (anterior/posterior [A/P], −0.2; medial/lateral [M/L], −1.0; dorsal/ventral [D/V], −2.4 to the bregma) of 2-month-old mice at a rate of 1 μl/min. After the injection, the needle was kept in place for 5 min, followed by suturing of the incision. i.v. injections of ASO (300 μg) were done into the tail vein. Three animals per group per time point were treated.

Western Blots

Tissue from the hippocampus and whole cortex of the left hemisphere of the brain was homogenized in radioimmunoprecipitation assay (RIPA) buffer. Protein samples were run on 4%–20% TGX Gels (Bio-Rad), transferred to polyvinylidene fluoride (PVDF) membranes (Millipore), and blotted using standard protocols. Primary antibodies were the following: HDAC2 (Abcam; ab12169) ACTIN (Abcam; ab3280), and BDNF (Abcam; ab108319). Bands shown in western blot images for these proteins were at the expected sizes of 55, 42, and 15 kDa, respectively. Secondary antibodies were goat anti-mouse infrared (IR) 680 (LI-COR Biosciences; #926-68020), goat anti-mouse IR 800 (LI-COR Biosciences; #926-32210), and goat anti-rabbit IR 800 (LI-COR Biosciences; #925-32211). Membranes were imaged on the LI-COR Biosciences Odyssey fluorescence imaging system.

Object Location Memory Test

Mice were habituated to an opaque polyurethane open box (10 × 10 × 12 in [x, y, z]) containing autoclaved bedding with one black line spatial cue for 3 days (5 min per day) prior to training. Mice were trained for 10 min with two 50-mL beakers in a particular location. Locomotion during the training session was tracked with ANY-Maze software. 24 h after training, one beaker was moved to a novel location, and the mice were recorded for 5 min. Interaction time with either object was scored, as previously described,[72] and exclusion criteria were applied, as previously described.[73] OLM was conducted on separate cohorts at 2 and 8 weeks. A subset of the 8-week cohort was used again for the 16-week OLM trial. The object that was moved to the novel location was altered at 16 weeks to help mitigate effects of retesting.

Total RNA-Seq

Tissue from the hippocampus and whole cortex of the right hemisphere was dissected. Total RNA and DNA was extracted with the AllPrep DNA/RNA/microRNA (miRNA) kit (QIAGEN). Total RNA-seq libraries were prepared using the TruSeq Stranded Total RNA Library Prep Kit with Ribo-Zero Gold (Illumina), according to the manufacturer's instructions. 1 μg of RNA was used as starting material and amplified with 12 PCR cycles. Library size distribution was checked

with an Agilent 2100 bioanalyzer, and quantity was determined using qPCR. Libraries were sequenced on an Illumina HiSeq 2500 using a 50-cycle rapid-run kit or an Illumina NextSeq instrument using a 75-cycle high-throughput kit. Read quality was confirmed with the FastQC tool, reads were aligned to the GRCm38.p3 mouse genome and transcriptome using TopHat,[74] and differential expression tests were performed using featureCounts[75] and edgeR,[76,77] with the glmLRT function used to determine significantly changed genes (false discovery rate [FDR] < 0.05). For determining the significance of *Hdac* isoform changes at each time point individually, differentially expressed genes were called with all time points present in the statistical model, and differentially expressed genes between SCR ASO- and *Hdac2* ASO1-treated animals were determined for each time point. Fold changes depicted for the isoform specificity graphs were calculated using the *Hdac* isoform fragments per kilobase of transcript per million mapped reads (FPKM), normalized to *Gapdh* FPKMs. Statistical analysis to identify differentially expressed genes during cognitive enhancement was conducted on combined time points of 2, 4, and 8 weeks after ICV (between times when OLM enhancement by *Hdac2* ASO1 relative to SCR ASO is significant). The contrast between SCR ASO and *Hdac2* ASO1 was determined using time point as a blocking variable. A minimum fold-change threshold of 25% was also applied. Database for Annotation, Visualization and Integrated Discovery (DAVID)[78,79] was used for functional annotation of genes. Animals used for OLM were later used for tissue analysis (except 3-day and 2-week animals, which were naive). At least 11 days elapsed between the behavioral assay and tissue collection. Elapsed days were equal for *Hdac2* ASO1 and SCR ASO animals to control for any long-term transcriptional changes elicited by the behavioral assay.

Analysis of Post-TES Signal

BedGraph files from total RNA sequencing experiments conducted in mouse primary neurons were downloaded from GenBank: GSE21161.[36] Fastq files of rat primary neuron polyA$^+$ and polyA$^-$ RNA-seq were downloaded from GenBank: GSE64988.[37] Hisat2[80] was used to align reads to the *Rattus norvegicus* genome assembly 5 (rn5) genome build. For visualization of the rn5-aligned gene tracks, bedtools[81] genomecov was used to create bedGraph files, which were scaled to read depth. Reads on each strand were extracted using the SAMtools[82] view specifying appropriate bitwise tags. Reference Sequence (RefSeq) annotated genes were used to generate an annotation of the +500- to +6,000-base pair region past the TES. When this region overlapped with another gene, the gene was removed from the annotation using bedtools intersect function with the –v option to exclude false interpretation of the signal that arises as the result of a nearby gene. Signal in the sense direction at these loci was extracted with SAMtools flagstat, and signal was normalized to the number of reads in the library. Signal from polyA$^+$ was subtracted from the polyA$^-$ sequencing experiments to remove any signal that came from incorrect annotation of the gene end site.

NRO

This procedure is based on several sources[39,40,83,84] and optimized to reduce nonspecific RNA binding. Nuclei were extracted as previously described,[40] with lysis buffer containing Igepal concentration, optimized based on cell type 0.25% for dN2a and 0.5% for primary neurons. The run-on reaction was done, as previously described.[40] RNA concentration was measured by NanoDrop and normalized. 30 μL Protein G Dynabeads were washed twice in BrU binding buffer, rotated at room temperature with 2 μg anti-bromodeoxyuridine (BrdU) antibody (Santa Cruz Biotechnology; IIB5, sc-32323) in BrU binding buffer for 10 min; blocking buffer was added, and beads rotated another 30 min at room temperature. After blocking, beads were washed 2 times with binding buffer. The blocked bead mixture was combined with RNA sample and put on a rotating stand for 30 min at room temperature. After binding, beads were washed twice for 2 min in BrU binding buffer, once in low-salt buffer and once in high-salt buffer and twice in Tris-EDTA-Triton X-100 (TET) buffer. Buffer compositions were previously published.[84] On the final TET wash, beads were moved to a new tube, TET was removed, and TRIzol was used to elute and purify RNA, as previously described.[83] Three rounds of immunoprecipitation were conducted on each sample. Purified RNA samples were heated at 65°C for 5 min and then placed on ice at least for 2 min prior to IP or reverse transcription reaction. Multiscribe reverse transcriptase was used to make cDNA, according to the manufacturer's recommendations.

To check for nonspecific RNA pull-down, the elution, after the third round of BrdU immunoprecipitation, was run on a bioanalyzer Eukaryote Total RNA Pico Series II chip, according to the manufacturer's instructions. NRO samples made with uridine triphosphate (UTP) were run in parallel to samples made with Bromo-UTP (BrUTP). Signal intensity is normalized across all samples in the gel-like output image.

Chromatin Immunoprecipitation

RNA Pol II ChIP cells were crosslinked with 0.5% formaldehyde in neurobasal for 10 min at room temperature. The crosslinking was stopped with glycine, and cells were immediately placed on ice and lysed in L1 buffer. Purification of chromatin was done as previously described.[40] Chromatin was sonicated in the Diagenode mini water bath to 100–400 bp fragments. 5 μg of antibody 3E8 (Millipore), 50 μL of protein G-coated Dynabeads, and 68 μg of chromatin were used per IP. Signal from intron 1 primers was standardized to input, normalizing to *Gapdh* intron 2 primers. Fold change was calculated relative to the SCR ASO signal from *Hdac2* exon 5 primer from each batch of chromatin. One-half of the plates were treated with SCR ASO and *Hdac2* ASO1 for each preparation of primary neurons, so batch effects could be taken into account.

Statistics

ANOVA and Student's t tests were conducted in GraphPad Prism version 8 with indicated post hoc tests.

SUPPLEMENTAL INFORMATION

Supplemental Information can be found online at https://doi.org/10.1016/j.omtn.2020.01.027.

AUTHOR CONTRIBUTIONS

C.B.G., S.G.P., K.A.G., A.J.K., T.P.M., and S.T.M. aided with experimental design and analysis. S.G.P. conducted sequencing prep and alignment. C.B.G. conducted *in vitro* assays, data analysis, and bioinformatics. K.A.G. was project manager for Vanderbilt University's team and conducted the tail-vein injection experiments. A.J.K. did ICV infusions. A.J.K and R.L.M. aided with expression analysis, animal behavior, and colony maintenance. R.L.M. conducted immunoblotting. H.B.K., H.Z., and E.E.S. designed and developed the *Hdac2*-targeting ASOs. S.B.G. designed and conducted experiments with the mouse *Fos* ASOs. S.G.P., J.D.S., T.P.M., and C.B.G. wrote the manuscript with assistance from all authors.

CONFLICTS OF INTEREST

S.T.M., S.G.P., and T.P.M. were Abbott Laboratories' employees when these experiments were conducted. H.B.K., H.Z., D.J.E., and E.E.S. are or were employees of Ionis Pharmaceuticals.

ACKNOWLEDGMENTS

We would like to thank Roger Colbran, Tim Broderick, and Bruce Howard for many helpful discussions. The authors sincerely appreciate help from Jane Wright, Garrett Kaas, and Joseph Weiss with primary neuron generation and isolation and help from Colin Fricker, Joseph Weiss, and Hero Haji with qPCR. We thank Benjamin Coleman and Joseph Weiss for their efforts in preliminary data generation. The views, opinions, and/or findings contained in this article are those of the authors and should not be interpreted as representing the official views or policies of the Department of Defense or the US government. Distribution Statement "A" (Approved for Public Release, Distribution Unlimited). All raw sequencing data generated in this study have been submitted to the NCBI Gene Expression Omnibus (GEO; https://www.ncbi.nlm.nih.gov/geo/) under accession number GenBank: GSE124726. All relevant data from this study are available on request from the corresponding authors (C.B.G. or T.P.M.). These studies were supported by grants from the NIH (MH091122 and MH57014 to J.D.S. and T32 MH065215) and Defense Advanced Research Projects Agency (HR0011-16-C-0065, HR0011-14-1-0001, HR0011-12-1-0015, and FA8650-13-C-7340), and start-up funds from Vanderbilt University.

REFERENCES

1. Stein, C.A., and Castanotto, D. (2017). FDA-Approved Oligonucleotide Therapies in 2017. Mol. Ther. *25*, 1069–1075.

2. Southwell, A.L., Skotte, N.H., Kordasiewicz, H.B., Østergaard, M.E., Watt, A.T., Carroll, J.B., Doty, C.N., Villanueva, E.B., Petoukhov, E., Vaid, K., et al. (2014). In vivo evaluation of candidate allele-specific mutant huntingtin gene silencing antisense oligonucleotides. Mol. Ther. *22*, 2093–2106.

3. Meng, L., Ward, A.J., Chun, S., Bennett, C.F., Beaudet, A.L., and Rigo, F. (2015). Towards a therapy for Angelman syndrome by targeting a long non-coding RNA. Nature *518*, 409–412.

4. Kordasiewicz, H.B., Stanek, L.M., Wancewicz, E.V., Mazur, C., McAlonis, M.M., Pytel, K.A., Artates, J.W., Weiss, A., Cheng, S.H., Shihabuddin, L.S., et al. (2012). Sustained therapeutic reversal of Huntington's disease by transient repression of huntingtin synthesis. Neuron *74*, 1031–1044.

5. Wu, H., Lima, W.F., Zhang, H., Fan, A., Sun, H., and Crooke, S.T. (2004). Determination of the role of the human RNase H1 in the pharmacology of DNA-like antisense drugs. J. Biol. Chem. *279*, 17181–17189.

6. Alter, J., Lou, F., Rabinowitz, A., Yin, H., Rosenfeld, J., Wilton, S.D., Partridge, T.A., and Lu, Q.L. (2006). Systemic delivery of morpholino oligonucleotide restores dystrophin expression bodywide and improves dystrophic pathology. Nat. Med. *12*, 175–177.

7. Sazani, P., Gemignani, F., Kang, S.H., Maier, M.A., Manoharan, M., Persmark, M., Bortner, D., and Kole, R. (2002). Systemically delivered antisense oligomers upregulate gene expression in mouse tissues. Nat. Biotechnol. *20*, 1228–1233.

8. Merkhofer, E.C., Hu, P., and Johnson, T.L. (2014). Introduction to cotranscriptional RNA splicing. Methods Mol. Biol. *1126*, 83–96.

9. Osheim, Y.N., Miller, O.L., Jr., and Beyer, A.L. (1985). RNP particles at splice junction sequences on Drosophila chorion transcripts. Cell *43*, 143–151.

10. Wu, Z.A., Murphy, C., Callan, H.G., and Gall, J.G. (1991). Small nuclear ribonucleoproteins and heterogeneous nuclear ribonucleoproteins in the amphibian germinal vesicle: loops, spheres, and snurposomes. J. Cell Biol. *113*, 465–483.

11. Beyer, A.L., Bouton, A.H., and Miller, O.L., Jr. (1981). Correlation of hnRNP structure and nascent transcript cleavage. Cell *26*, 155–165.

12. Alarcón, J.M., Malleret, G., Touzani, K., Vronskaya, S., Ishii, S., Kandel, E.R., and Barco, A. (2004). Chromatin acetylation, memory, and LTP are impaired in CBP+/- mice: a model for the cognitive deficit in Rubinstein-Taybi syndrome and its amelioration. Neuron *42*, 947–959.

13. Korzus, E., Rosenfeld, M.G., and Mayford, M. (2004). CBP histone acetyltransferase activity is a critical component of memory consolidation. Neuron *42*, 961–972.

14. Wood, M.A., Kaplan, M.P., Park, A., Blanchard, E.J., Oliveira, A.M., Lombardi, T.L., and Abel, T. (2005). Transgenic mice expressing a truncated form of CREB-binding protein (CBP) exhibit deficits in hippocampal synaptic plasticity and memory storage. Learn. Mem. *12*, 111–119.

15. Levenson, J.M., O'Riordan, K.J., Brown, K.D., Trinh, M.A., Molfese, D.L., and Sweatt, J.D. (2004). Regulation of histone acetylation during memory formation in the hippocampus. J. Biol. Chem. *279*, 40545–40559.

16. Hawk, J.D., Florian, C., and Abel, T. (2011). Post-training intrahippocampal inhibition of class I histone deacetylases enhances long-term object-location memory. Learn. Mem. *18*, 367–370.

17. Guan, J.S., Haggarty, S.J., Giacometti, E., Dannenberg, J.H., Joseph, N., Gao, J., Nieland, T.J., Zhou, Y., Wang, X., Mazitschek, R., et al. (2009). HDAC2 negatively regulates memory formation and synaptic plasticity. Nature *459*, 55–60.

18. McQuown, S.C., Barrett, R.M., Matheos, D.P., Post, R.J., Rogge, G.A., Alenghat, T., Mullican, S.E., Jones, S., Rusche, J.R., Lazar, M.A., and Wood, M.A. (2011). HDAC3 is a critical negative regulator of long-term memory formation. J. Neurosci. *31*, 764–774.

19. Morris, M.J., Mahgoub, M., Na, E.S., Pranav, H., and Monteggia, L.M. (2013). Loss of histone deacetylase 2 improves working memory and accelerates extinction learning. J. Neurosci. *33*, 6401–6411.

20. Norwood, J., Franklin, J.M., Sharma, D., and D'Mello, S.R. (2014). Histone deacetylase 3 is necessary for proper brain development. J. Biol. Chem. *289*, 34569–34582.

21. Choubey, S.K., and Jeyakanthan, J. (2018). Molecular dynamics and quantum chemistry-based approaches to identify isoform selective HDAC2 inhibitor - a novel target to prevent Alzheimer's disease. J. Recept. Signal Transduct. Res. *38*, 266–278.

22. Wang, D.F., Helquist, P., Wiech, N.L., and Wiest, O. (2005). Toward selective histone deacetylase inhibitor design: homology modeling, docking studies, and molecular dynamics simulations of human class I histone deacetylases. J. Med. Chem. *48*, 6936–6947.

23. Yamakawa, H., Cheng, J., Penney, J., Gao, F., Rueda, R., Wang, J., Yamakawa, S., Kritskiy, O., Gjoneska, E., and Tsai, L.H. (2017). The Transcription Factor Sp3 Cooperates with HDAC2 to Regulate Synaptic Function and Plasticity in Neurons. Cell Rep. *20*, 1319–1334.

24. Kennedy, A.J., Rahn, E.J., Paulukaitis, B.S., Savell, K.E., Kordasiewicz, H.B., Wang, J., Lewis, J.W., Posey, J., Strange, S.K., Guzman-Karlsson, M.C., et al. (2016). Tcf4 Regulates Synaptic Plasticity, DNA Methylation, and Memory Function. Cell Rep. *16*, 2666–2685.

25. Penney, J., and Tsai, L.H. (2014). Histone deacetylases in memory and cognition. Sci. Signal. *7*, re12.

26. El-Brolosy, M.A., and Stainier, D.Y.R. (2017). Genetic compensation: A phenomenon in search of mechanisms. PLoS Genet. *13*, e1006780.

27. Lian, H., Roy, E., and Zheng, H. (2016). Protocol for Primary Microglial Culture Preparation. Bio. Protoc. *6*, e1989.

28. Saura, J. (2007). Microglial cells in astroglial cultures: a cautionary note. J. Neuroinflammation *4*, 26.

29. Geary, R.S., Norris, D., Yu, R., and Bennett, C.F. (2015). Pharmacokinetics, biodistribution and cell uptake of antisense oligonucleotides. Adv. Drug Deliv. Rev. *87*, 46–51.

30. Cossum, P.A., Sasmor, H., Dellinger, D., Truong, L., Cummins, L., Owens, S.R., Markham, P.M., Shea, J.P., and Crooke, S. (1993). Disposition of the 14C-labeled phosphorothioate oligonucleotide ISIS 2105 after intravenous administration to rats. J. Pharmacol. Exp. Ther. *267*, 1181–1190.

31. Smith, R.A., Miller, T.M., Yamanaka, K., Monia, B.P., Condon, T.P., Hung, G., Lobsiger, C.S., Ward, C.M., McAlonis-Downes, M., Wei, H., et al. (2006). Antisense oligonucleotide therapy for neurodegenerative disease. J. Clin. Invest. *116*, 2290–2296.

32. Marin, I., and Kipnis, J. (2013). Learning and memory ... and the immune system. Learn. Mem. *20*, 601–606.

33. Calabrese, F., Rossetti, A.C., Racagni, G., Gass, P., Riva, M.A., and Molteni, R. (2014). Brain-derived neurotrophic factor: a bridge between inflammation and neuroplasticity. Front. Cell. Neurosci. *8*, 430.

34. Guan, Z., and Fang, J. (2006). Peripheral immune activation by lipopolysaccharide decreases neurotrophins in the cortex and hippocampus in rats. Brain Behav. Immun. *20*, 64–71.

35. Schnydrig, S., Korner, L., Landweer, S., Ernst, B., Walker, G., Otten, U., and Kunz, D. (2007). Peripheral lipopolysaccharide administration transiently affects expression of brain-derived neurotrophic factor, corticotropin and proopiomelanocortin in mouse brain. Neurosci. Lett. *429*, 69–73.

36. Kim, T.K., Hemberg, M., Gray, J.M., Costa, A.M., Bear, D.M., Wu, J., Harmin, D.A., Laptewicz, M., Barbara-Haley, K., Kuersten, S., et al. (2010). Widespread transcription at neuronal activity-regulated enhancers. Nature *465*, 182–187.

37. Savell, K.E., Gallus, N.V., Simon, R.C., Brown, J.A., Revanna, J.S., Osborn, M.K., Song, E.Y., O'Malley, J.J., Stackhouse, C.T., Norvil, A., et al. (2016). Extra-coding RNAs regulate neuronal DNA methylation dynamics. Nat. Commun. *7*, 12091.

38. Di Ruscio, A., Ebralidze, A.K., Benoukraf, T., Amabile, G., Goff, L.A., Terragni, J., Figueroa, M.E., De Figueiredo Pontes, L.L., Alberich-Jorda, M., Zhang, P., et al. (2013). DNMT1-interacting RNAs block gene-specific DNA methylation. Nature *503*, 371–376.

39. Kim, Y.J., Greer, C.B., Cecchini, K.R., Harris, L.N., Tuck, D.P., and Kim, T.H. (2013). HDAC inhibitors induce transcriptional repression of high copy number genes in breast cancer through elongation blockade. Oncogene *32*, 2828–2835.

40. Greer, C.B., Tanaka, Y., Kim, Y.J., Xie, P., Zhang, M.Q., Park, I.H., and Kim, T.H. (2015). Histone Deacetylases Positively Regulate Transcription through the Elongation Machinery. Cell Rep. *13*, 1444–1455.

41. Yu, M., Yang, W., Ni, T., Tang, Z., Nakadai, T., Zhu, J., and Roeder, R.G. (2015). RNA polymerase II-associated factor 1 regulates the release and phosphorylation of paused RNA polymerase II. Science *350*, 1383–1386.

42. Rahl, P.B., Lin, C.Y., Seila, A.C., Flynn, R.A., McCuine, S., Burge, C.B., Sharp, P.A., and Young, R.A. (2010). c-Myc regulates transcriptional pause release. Cell *141*, 432–445.

43. Phatnani, H.P., and Greenleaf, A.L. (2006). Phosphorylation and functions of the RNA polymerase II CTD. Genes Dev. *20*, 2922–2936.

44. Komarnitsky, P., Cho, E.J., and Buratowski, S. (2000). Different phosphorylated forms of RNA polymerase II and associated mRNA processing factors during transcription. Genes Dev. *14*, 2452–2460.

45. Amin, S.A., Adhikari, N., Kotagiri, S., Jha, T., and Ghosh, B. (2019). Histone deacetylase 3 inhibitors in learning and memory processes with special emphasis on benzamides. Eur. J. Med. Chem. *166*, 369–380.

46. Qin, L., Ma, K., Wang, Z.J., Hu, Z., Matas, E., Wei, J., and Yan, Z. (2018). Social deficits in Shank3-deficient mouse models of autism are rescued by histone deacetylase (HDAC) inhibition. Nat. Neurosci. *21*, 564–575.

47. Gräff, J., Rei, D., Guan, J.S., Wang, W.Y., Seo, J., Hennig, K.M., Nieland, T.J., Fass, D.M., Kao, P.F., Kahn, M., et al. (2012). An epigenetic blockade of cognitive functions in the neurodegenerating brain. Nature *483*, 222–226.

48. Rigo, F., Chun, S.J., Norris, D.A., Hung, G., Lee, S., Matson, J., Fey, R.A., Gaus, H., Hua, Y., Grundy, J.S., et al. (2014). Pharmacology of a central nervous system delivered 2′-O-methoxyethyl-modified survival of motor neuron splicing oligonucleotide in mice and nonhuman primates. J. Pharmacol. Exp. Ther. *350*, 46–55.

49. McCampbell, A., Cole, T., Wegener, A.J., Tomassy, G.S., Setnicka, A., Farley, B.J., Schoch, K.M., Hoye, M.L., Shabsovich, M., Sun, L., et al. (2018). Antisense oligonucleotides extend survival and reverse decrement in muscle response in ALS models. J. Clin. Invest. *128*, 3558–3567.

50. Adams, J.P., and Sweatt, J.D. (2002). Molecular psychology: roles for the ERK MAP kinase cascade in memory. Annu. Rev. Pharmacol. Toxicol. *42*, 135–163.

51. Peng, S., Zhang, Y., Zhang, J., Wang, H., and Ren, B. (2010). ERK in learning and memory: a review of recent research. Int. J. Mol. Sci. *11*, 222–232.

52. Nelson, P.A., Sage, J.R., Wood, S.C., Davenport, C.M., Anagnostaras, S.G., and Boulanger, L.M. (2013). MHC class I immune proteins are critical for hippocampus-dependent memory and gate NMDAR-dependent hippocampal long-term depression. Learn. Mem. *20*, 505–517.

53. Ru, M., and Liu, H. (2018). Association between Y-Maze Acquisition Learning and Major Histocompatibility Complex Class II Polymorphisms in Mice. BioMed Res. Int. *2018*, 6381932.

54. Fuerst, P.G., Koizumi, A., Masland, R.H., and Burgess, R.W. (2008). Neurite arborization and mosaic spacing in the mouse retina require DSCAM. Nature *451*, 470–474.

55. Golan, H., Levav, T., Mendelsohn, A., and Huleihel, M. (2004). Involvement of tumor necrosis factor alpha in hippocampal development and function. Cereb. Cortex *14*, 97–105.

56. O'Brien, R.J., Xu, D., Petralia, R.S., Steward, O., Huganir, R.L., and Worley, P. (1999). Synaptic clustering of AMPA receptors by the extracellular immediate-early gene product Narp. Neuron *23*, 309–323.

57. Stevens, B., Allen, N.J., Vazquez, L.E., Howell, G.R., Christopherson, K.S., Nouri, N., Micheva, K.D., Mehalow, A.K., Huberman, A.D., Stafford, B., et al. (2007). The classical complement cascade mediates CNS synapse elimination. Cell *131*, 1164–1178.

58. Goddard, C.A., Butts, D.A., and Shatz, C.J. (2007). Regulation of CNS synapses by neuronal MHC class I. Proc. Natl. Acad. Sci. USA *104*, 6828–6833.

59. Stellwagen, D., Beattie, E.C., Seo, J.Y., and Malenka, R.C. (2005). Differential regulation of AMPA receptor and GABA receptor trafficking by tumor necrosis factor-alpha. J. Neurosci. *25*, 3219–3228.

60. Kiryushko, D., Novitskaya, V., Soroka, V., Klingelhofer, J., Lukanidin, E., Berezin, V., and Bock, E. (2006). Molecular mechanisms of Ca(2+) signaling in neurons induced by the S100A4 protein. Mol. Cell. Biol. *26*, 3625–3638.

61. Dmytriyeva, O., Pankratova, S., Owczarek, S., Sonn, K., Soroka, V., Ridley, C.M., Marsolais, A., Lopez-Hoyos, M., Ambartsumian, N., Lukanidin, E., et al. (2012). The metastasis-promoting S100A4 protein confers neuroprotection in brain injury. Nat. Commun. *3*, 1197.

62. Pankratova, S., Klingelhofer, J., Dmytriyeva, O., Owczarek, S., Renziehausen, A., Syed, N., Porter, A.E., Dexter, D.T., and Kiryushko, D. (2018). The S100A4 Protein Signals through the ErbB4 Receptor to Promote Neuronal Survival. Theranostics *8*, 3977–3990.

63. Hagmeyer, S., Romão, M.A., Cristóvão, J.S., Vilella, A., Zoli, M., Gomes, C.M., and Grabrucker, A.M. (2019). Distribution and Relative Abundance of S100 Proteins in the Brain of the APP23 Alzheimer's Disease Model Mice. Front. Neurosci. *13*, 640.

64. Tian, Z.Y., Wang, C.Y., Wang, T., Li, Y.C., and Wang, Z.Y. (2019). Glial S100A6 Degrades β-amyloid Aggregation through Targeting Competition with Zinc Ions. Aging Dis. *10*, 756–769.

65. Donato, R., Cannon, B.R., Sorci, G., Riuzzi, F., Hsu, K., Weber, D.J., and Geczy, C.L. (2013). Functions of S100 proteins. Curr. Mol. Med. *13*, 24–57.

66. Beswick, E.J., and Reyes, V.E. (2009). CD74 in antigen presentation, inflammation, and cancers of the gastrointestinal tract. World J. Gastroenterol. *15*, 2855–2861.

67. Kiyota, T., Zhang, G., Morrison, C.M., Bosch, M.E., Weir, R.A., Lu, Y., Dong, W., and Gendelman, H.E. (2015). AAV2/1 CD74 Gene Transfer Reduces β-amyloidosis and Improves Learning and Memory in a Mouse Model of Alzheimer's Disease. Mol. Ther. *23*, 1712–1721.

68. DeVos, S.L., and Miller, T.M. (2013). Antisense oligonucleotides: treating neurodegeneration at the level of RNA. Neurotherapeutics *10*, 486–497.

69. Mousavi, K., Zare, H., Dell'orso, S., Grontved, L., Gutierrez-Cruz, G., Derfoul, A., Hager, G.L., and Sartorelli, V. (2013). eRNAs promote transcription by establishing chromatin accessibility at defined genomic loci. Mol. Cell *51*, 606–617.

70. Gaj, T., Gersbach, C.A., and Barbas, C.F., 3rd (2013). ZFN, TALEN, and CRISPR/Cas-based methods for genome engineering. Trends Biotechnol. *31*, 397–405.

71. Livak, K.J., and Schmittgen, T.D. (2001). Analysis of relative gene expression data using real-time quantitative PCR and the 2(-Delta Delta C(T)) Method. Methods *25*, 402–408.

72. Haettig, J., Stefanko, D.P., Multani, M.L., Figueroa, D.X., McQuown, S.C., and Wood, M.A. (2011). HDAC inhibition modulates hippocampus-dependent long-term memory for object location in a CBP-dependent manner. Learn. Mem. *18*, 71–79.

73. Vogel-Ciernia, A., and Wood, M.A. (2014). Examining object location and object recognition memory in mice. Curr. Protoc. Neurosci. *69*, 8.31.1–8.31.17.

74. Trapnell, C., Pachter, L., and Salzberg, S.L. (2009). TopHat: discovering splice junctions with RNA-Seq. Bioinformatics *25*, 1105–1111.

75. Liao, Y., Smyth, G.K., and Shi, W. (2014). featureCounts: an efficient general purpose program for assigning sequence reads to genomic features. Bioinformatics *30*, 923–930.

76. Robinson, M.D., McCarthy, D.J., and Smyth, G.K. (2010). edgeR: a Bioconductor package for differential expression analysis of digital gene expression data. Bioinformatics *26*, 139–140.

77. McCarthy, D.J., Chen, Y., and Smyth, G.K. (2012). Differential expression analysis of multifactor RNA-Seq experiments with respect to biological variation. Nucleic Acids Res. *40*, 4288–4297.

78. Huang, W., Sherman, B.T., and Lempicki, R.A. (2009). Systematic and integrative analysis of large gene lists using DAVID bioinformatics resources. Nat. Protoc. *4*, 44–57.

79. Huang, W., Sherman, B.T., and Lempicki, R.A. (2009). Bioinformatics enrichment tools: paths toward the comprehensive functional analysis of large gene lists. Nucleic Acids Res. *37*, 1–13.

80. Kim, D., Langmead, B., and Salzberg, S.L. (2015). HISAT: a fast spliced aligner with low memory requirements. Nat. Methods *12*, 357–360.

81. Quinlan, A.R., and Hall, I.M. (2010). BEDTools: a flexible suite of utilities for comparing genomic features. Bioinformatics *26*, 841–842.

82. Li, H., Handsaker, B., Wysoker, A., Fennell, T., Ruan, J., Homer, N., Marth, G., Abecasis, G., and Durbin, R.; 1000 Genome Project Data Processing Subgroup (2009). The Sequence Alignment/Map format and SAMtools. Bioinformatics *25*, 2078–2079.

83. Roberts, T.C., Hart, J.R., Kaikkonen, M.U., Weinberg, M.S., Vogt, P.K., and Morris, K.V. (2015). Quantification of nascent transcription by bromouridine immunocapture nuclear run-on RT-qPCR. Nat. Protoc. *10*, 1198–1211.

84. Core, L.J., Waterfall, J.J., and Lis, J.T. (2008). Nascent RNA sequencing reveals widespread pausing and divergent initiation at human promoters. Science *322*, 1845–1848.